

BSA and HSA protein amyloid aggregates: Comparison and design for potential applications

Sonalika Maurya
(BO12M1007)

A Dissertation Submitted to
Indian Institute of Technology Hyderabad
In Partial Fulfilment of the Requirements for
The Degree of Master of Technology



भारतीय प्रौद्योगिकी संस्थान हैदराबाद
Indian Institute of Technology Hyderabad

Department of Biotechnology

June, 2014

Declaration

I declare that this written submission represents my ideas in my own words, and where others' ideas or words have been included, I have adequately cited and referenced the original sources. I also declare that I have adhered to all principles of academic honesty and integrity and have not misrepresented or fabricated or falsified any idea/data/fact/source in my submission. I understand that any violation of the above will be a cause for disciplinary action by the Institute and can also evoke penal action from the sources that have thus not been properly cited, or from whom proper permission has not been taken when needed.

Sonalika Maurya
BO12M1007

Approval Sheet

This thesis entitled "*BSA and HSA protein amyloid aggregates: comparison and design for potential applications*" by Sonalika Maurya is approved for the degree of Master of Technology from IIT Hyderabad.

Dr. Basant K. Patel

(Thesis Advisor)

Department of Biotechnology

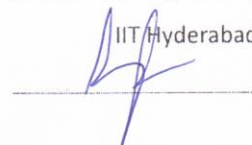
IIT Hyderabad



Dr. Parag Pawar

Department of Chemical Engineering

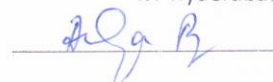
IIT Hyderabad



Dr. Anindya Roy

Department of Biotechnology

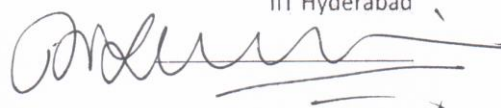
IIT Hyderabad



Dr. T. Rathinavelan

Department of Biotechnology

IIT Hyderabad



Acknowledgements

With deep regards and profound respect, I avail the opportunity to express my deep sense of gratitude to my supervisor Dr. Basant Kumar Patel for his inspiring guidance, constant encouragement and support throughout the period of the M.Tech thesis work. I also acknowledge my sincere regards to the rest of my thesis committee: Dr. Anindya Roy, Dr. T. Rathinavelan and Dr. Parag Pawar for their insightful comments, challenging questions and valuable suggestions.

I would like to add a special note of thanks to my senior lab mates, Vishwanath Sivlingam, Archana Prasad, Neetu Sharma and my colleague Lakshmi Prasanna for their kind help and support whenever it was required.

Last but not the least, I express my deep sense of gratitude to my loving Parents, for selflessly extending their ceaseless help and moral support at all times.

ABSTRACT

Protein mis-folding and aggregation result in many human diseases and some of these diseases are caused when the protein aggregation leads to amyloid formation (Chiti and Dobson, 2006). Amyloids are insoluble, fibrous and well organized protein aggregates having cross- β core structure (Chiti and Dobson, 2006, Nelson et al., 2005). Some of the examples of amyloid-associated diseases include: Alzheimer's disease, Prion disease, and Huntington's disease. The all- α helix, acidic and multi-domain proteins bovine serum albumin (BSA) and Human serum albumin (HSA) can also form amyloid aggregates *in vitro* at high temperatures (Holm et al., 2007, Juarez et al., 2009a). BSA and HSA have multi-functional *in vivo* roles like delivering major nutrients to the cells and isolating toxins from the cells as they possess many ligand binding sites. They have half-life of 19 days and ability to restore plasma (Wunder et al., 2003). These proteins have one free cysteine and share over 76% sequence similarity (Francis, 2010) (Huang et al., 2004). Recently, these proteins have been used as a plasma expander and also as preferred drug delivery agents (Park, 2012). Amyloid aggregates can be either cytotoxic causing disease or they can be beneficial or functional in some cases. BSA/HSA amyloid aggregates are shown to be non-cytotoxic (Holm et al., 2007) and are not involved in causing amyloid diseases, thus a better understanding of their amyloid properties can help in finding any potential applications. The present work undertakes a comparative analysis of properties of BSA and HSA protein amyloid aggregates. It is found here that despite the very high sequence similarity and similar biochemical properties, the amyloid aggregates of BSA and HSA vary significantly in their properties and stabilities. Previously, conjugation of therapeutic proteins (eg. Interferon alfa 2b & human growth hormone) with HSA has been shown to increase their circulatory life span and hence their therapeutic period. Here, we hypothesized that conjugating a therapeutic protein or peptide to amyloid form of HSA would further extend the circulatory life as the amyloid clearance is expectedly slower. As a proof of the feasibility, we succeeded in cross-linking two HSA molecules *via* their one free-cysteine residues followed by converting them into amyloid-like aggregates. Further studies using amyloid converted heterodimer of HSA with a therapeutic protein could lead to potential applications if the hetero-dimer aggregates remain non-cytotoxic.

Abbreviations

BSA	Bovine serum albumin
HSA	Human serum albumin
SDS	Sodium dodecyl sulphate
Sarkosyl	Sodium lauroyl sarcosinate
RT	Room temperature
R	Reducing condition
NR	Non-reducing condition
SDD-AGE	Semi-denaturing detergent agarose gel electrophoresis
SDS-PAGE	Sodium dodecyl sulphate-polyacrylamide gel electrophoresis
DTNB	5, 5'-dithio-bis (2-nitrobenzoic acid)
DTT	Dithiothreitol
Th-T	Thioflavin-T
CR	Congo red
NaCl	Sodium chloride
H ₂ O ₂	Hydrogen peroxide
EPR	Enhanced permeability and retention effect
SEC	Size exclusion chromatography

Contents

Declaration	2
Approval Sheet	3
Acknowledgements	4
Abstract	5
Abbreviations	6
1. Introduction	9-17
1.1 Amyloid aggregates	9-11
1.2 Amyloidosis	11-13
1.3 Functional amyloid aggregates	13
1.4 Amyloid aggregate forming proteins	14
1.4.1 BSA & HSA: Amyloid aggregate forming proteins	14-15
1.4.2 BSA & HSA form amyloid aggregates	16
1.4.3 Aggregation pathways of serum albumins	16-17
2. Materials and Methods	18-22
2.1 Materials	18
2.2 Preparation of BSA & HSA amyloid aggregates	18
2.3 Confirmatory assays for amyloid formation	18
2.3.1 Thioflavin-T dye binding assay	18
2.3.2 Congo red dye binding assay	18-19
2.3.3 Intrinsic tryptophan fluorescence	19
2.3.4 Test for self-seeding of BSA /HSA amyloid aggregates	19
2.4 Amyloid Stability assays	19
2.4.1 Comparison of detergent stability of BSA and HSA amyloid aggregates	19-20
2.4.2 Comparative pH stability of BSA and HSA amyloid aggregates	20
2.4.3 Comparative stability of BSA & HSA amyloid aggregates at pH 6.0 & 40°C	20
2.5 Disulphide linked conjugation using free cysteine to get homo-dimers of BSA/HSA	21
2.5.1 Estimation of free sulphhydryl group of BSA & HSA by Ellman's reagent assay	21
2.5.2 Induced disulphide linked dimerization of BSA & HSA using H ₂ O ₂	21
2.5.3 Purification of homo-dimer of HSA/BSA by size exclusion chromatography	21-22

3. Results and Discussion	23-40
3.1 In-vitro formation of BSA and HSA protein amyloid aggregates	23
3.2 Confirmatory assays of BSA and HSA protein amyloid aggregates	23-27
3.2.1 BSA and HSA amyloid aggregation detected by Thioflavin-T dye binding assay	23-24
3.2.2 BSA and HSA amyloid aggregation detected by Congo red dye binding assay	24-25
3.2.3 Intrinsic tryptophan fluorescence of BSA and HSA amyloid aggregates	25-26
3.2.4 Self-seeding at sub-optimal temperature of BSA and HSA	26-27
3.3 Comparative stability assays of BSA and HSA amyloid aggregates	27-34
3.3.1 Detergent stability by SDD-AGE	27-29
3.3.2 The pH stability of BSA and HSA amyloid aggregates	29-32
3.3.3 Comparative stability of BSA and HSA amyloid aggregates at pH6.0 & 40°C	32-34
3.4 Conjugation using free cysteine to obtain homo-dimer of BSA & HSA	35-40
3.4.1 Estimation of free sulphhydryl group of BSA & HSA	35
3.4.2 Disulphide linked homo-dimerization of BSA & HSA	35-36
3.4.3 Separation of monomer & dimer of BSA & HSA by FPLC	36-38
3.4.4 HSA-dimer fibrillization and its confirmatory assays	38-40
4. Conclusion	41
References	42-44

CHAPTER I INTRODUCTION

1.1 Amyloid aggregates

Many human diseases are as a result of protein misfolding and aggregation. Some of these diseases are caused due to protein aggregation in an amyloid form (Chiti and Dobson, 2006). Amyloids are unbranched, fibrillar, rigid, insoluble, highly organized and protease-resistant aggregates of proteins (Chiti and Dobson, 2006). These are approximately 75-100 Å in diameter.

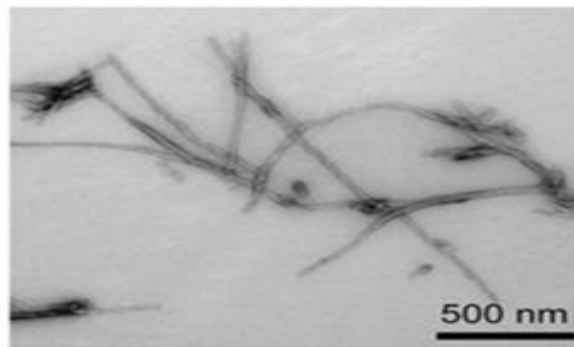


Figure 1: Typical morphology of amyloid fibrils observed under electron microscope (Sunde and Blake, 1997).

They have characteristic “cross β -sheet” structure, revealed by X-ray diffraction studies, where the β -sheets are parallel to the axis of the fibril but β -strands are perpendicular to the fiber axis and hence the name cross- β (Nelson et al., 2005) (**Figure 2**).

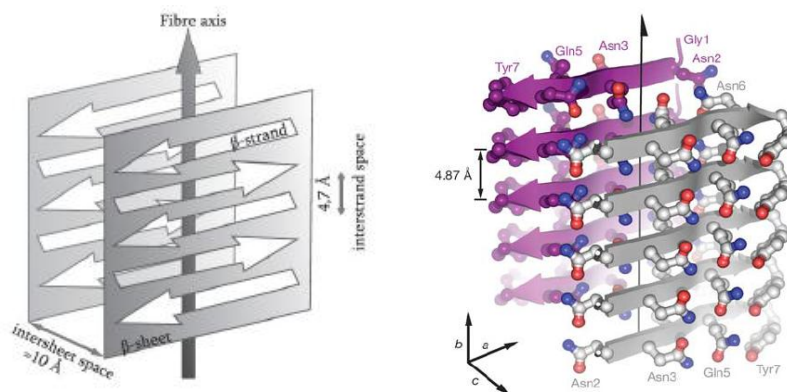


Figure 2: Cross-beta structure present in amyloids (Nelson et al., 2005).

Amyloids differ from other fibrillar structures like collagen or silk fibroin in their ability to bind the dye Congo red and exhibit bright apple green birefringence when viewed under polarized light (**Figure 3**), and also in their ability to bind the dye Thioflavin T thereby exhibiting bright fluorescence

(Figure 4) (LeVine, 1993). Amyloid aggregates are partially stable against protease (eg. proteinase K) and even ionic detergents like SDS and sodium lauroyl sarcosinate at room temperature.

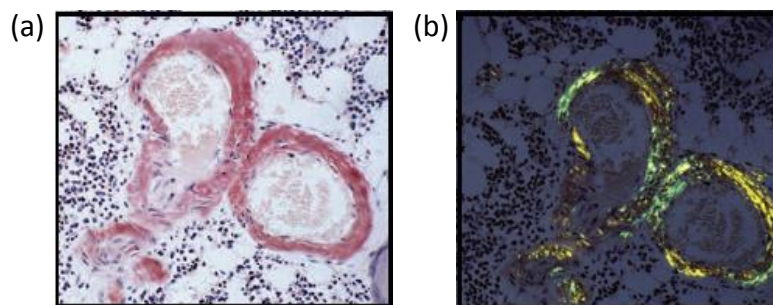


Figure 3: (a) Red in Bright field microscopy (b) Bright apple green birefringence in Polarized light microscopy (Merlini and Bellotti, 2003).

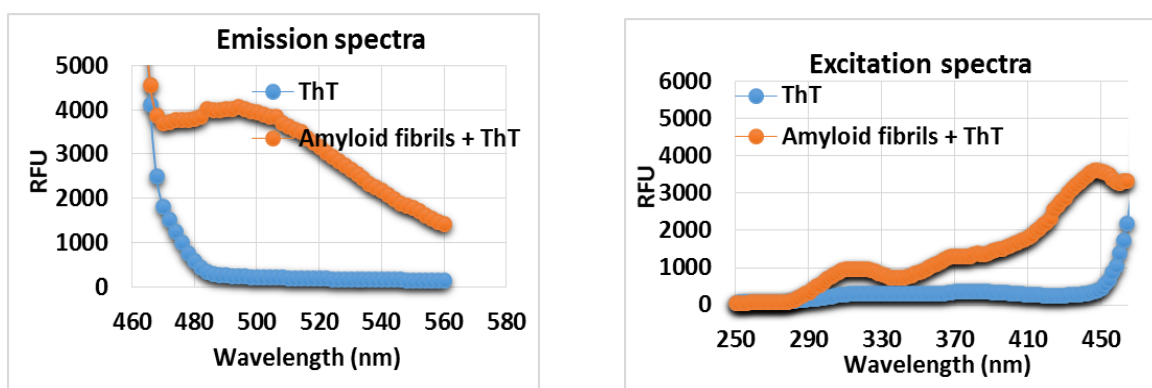


Figure 4: Characteristic increase in ThT fluorescence upon binding to amyloid fibrils.

Amyloid formation is a nucleation dependent process (Figure 5a & b). The rate of growth of amyloid fibres is increased by the presence of even small amounts of pre-formed aggregates which act as seed. This process is known as seeding (Figure 6) and it bears resemblance to crystal growth of proteins or salts which can also be seeded by pre-formed crystals.

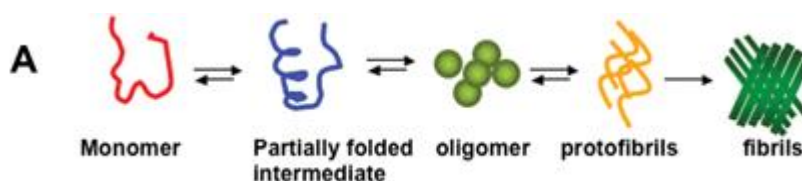


Figure 5: (a) Schematic of Amyloid aggregation.

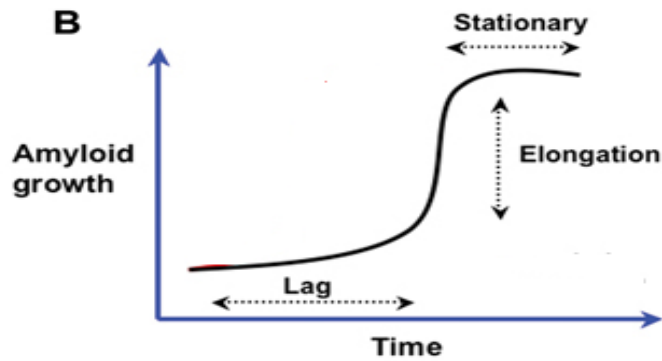


Figure 5: (B) Amyloid formation by nucleation dependent polymerization mechanism (Sunde and Blake, 1997).

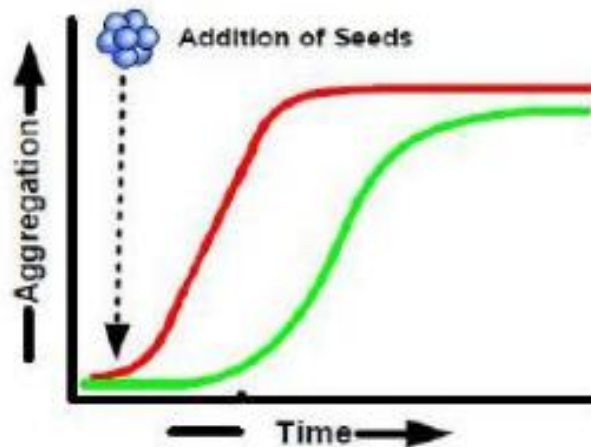


Figure 6: Nucleation-dependent polymerization model of amyloid aggregation (Kumar and Walter, 2011).

As expected, the process of seeding leads to reduction in the lag period preceding the amyloid growth and thus the amyloid growth curve shift toward left of the unseeded growth curve.

1.2 Amyloidosis

Amyloidosis is a pathological state associated with the deposition of conformationally altered proteins in the amyloid state, generally in the extracellular spaces of organs or tissues (Pepys, 2006) (called plaques or amyloid fibrils) but also sometimes as intracellular “inclusions bodies”. The most well-known neurodegenerative disease caused due to amyloid deposits is the Alzheimer’s disease where the deposition of $A\beta$ 1-40 peptide fragments happens in brain. Parkinson’s and Huntington’s diseases are also amyloid diseases and are caused by the aggregation of α -synuclein and huntingtin protein respectively (Chiti and Dobson, 2006).

Amyloid deposition can be in a systemic or localized pattern. When the amyloid is restricted to a particular organ or tissue, it is called a localized amyloidosis. When the amyloid depositions are found in many or all of the body regions the disease is called systemic amyloidosis. Amyloid deposition can occur in organs such as kidneys, spleen, heart, muscles, brain or even blood vessels. Furthermore, amyloidosis can be familial (hereditary) or acquired. Acquired amyloid disease can develop due to the aggravation of an already present diseased state in an individual, whereby there is an increase in the amount of proteins with amyloid characteristics. Example- secondary reactive amyloidosis, which occurs due to aggregation of the serum amyloid A protein, secreted during acute phase inflammation arising as a result of a primary disease conditions, like rheumatoid arthritis or tuberculosis (Merlini and Bellotti, 2003). Hereditary or familial amyloidosis occur due to the deposition of an altered protein encoded by a mutated gene. Example- Fibrinogen amyloidosis occurs due to mutations in the fifth exon region of the fibrinogen α chain encoding gene (Kang et al., 2005).

Amyloid aggregates can become cytotoxic by permeabilizing the cell membrane thereby leading to increase in cytosolic free calcium (Ca^{2+} dyshomeostasis) (Demuro et al., 2005). The increase in Ca^{2+} level in mitochondrial matrix results in reactive oxygen species production, cytochrome c release, altered signalling pathway, and finally mitochondria dysfunction occurs. Amyloidosis can be also grouped into neurodegenerative amyloidosis, non-neuropathic localized amyloidosis and non-neuropathic systemic amyloidosis (Chiti and Dobson, 2006). In neurodegenerative amyloidosis, aggregation occurs in the brain as found in Alzheimer's disease, Parkinson's disease and Huntington's disease. In non-neuropathic localized amyloidosis, aggregation occurs in a single type of tissue as in the case of AL amyloidosis. In non-neuropathic systemic amyloidosis, aggregation occurs in multiple tissues as found to be in atrial amyloidosis, pulmonary alveolar proteinosis, and fibrinogen amyloidosis. (Chiti and Dobson, 2006). List of Amyloid associated diseases is given in

Table 1.

Table 1: List of amyloid associated diseases (Chiti and Dobson, 2006).

	Amyloid disease	Protein
Neurodegenerative diseases	Alzheimer's disease	A β peptide
	Parkinson's disease	α -Synuclein
	Huntington's disease	Huntingtin with polyQ expansion
	Familial British dementia	ABri
	Spinocerebellar ataxias	Ataxins with polyQ expansion
Non-neuropathic systemic amyloidoses	Primary systemic amyloidosis	Immunoglobulin light chain
	Ig-heavy chain associated amyloidosis	Immunoglobulin heavy chain
	Hemodialysis-related amyloidosis	β_2 -microglobulin
	Senile systemic amyloidosis	Transthyretin
	Hereditary systemic ApoAI amyloidosis	Apolipoprotein AI
	Hereditary systemic ApoAII amyloidosis	Apolipoprotein AII
	Hereditary lysozyme amyloidosis	Lysozyme
Non-neuropathic localized diseases	Atrial amyloidosis	Atrial natriuretic factor
	Injection-localized amyloidosis	Insulin
	Pulmonary alveolar proteinosis	Lung surfactant protein C
	Senile seminal vesicle amyloidosis	Semenogelin I
Prion diseases	Spongiform encephalopathies, Creutzfeldt-Jakob disease and Kuru	PrP

1.3 Functional amyloid aggregates

Formation of amyloid structure has been hypothesized as an inherent or generic property of every polypeptide chain (Polverino de Laureto et al., 2003). All Amyloids are not cytotoxic and some amyloid like structures are also present naturally which do not cause diseases. In fact, some amyloids are called "functional amyloids" as they may have beneficial role. For example: The *E.coli* have a protein called curlin which forms amyloid structures and helps the organism to colonize on inert surfaces and mediate binding to host proteins. Also, the fungus *Neurospora crassa* secrete hydrophobins which are amyloid forming proteins that lower the water surface tension and allow the development of aerial hyphae. Furthermore, the silk fibers of the spider web are amyloid structures of the protein spidroin (Chiti and Dobson, 2006). Some other functional amyloids include: chaplins (*Streptomyces coelicolor*), hydrophobin EAS (*Neurospora crassa*), proteins of chorion of the eggshell (*Bombyx mori*), intraluminal domain of Pmel17 (*Homo sapiens*), Ure2p (*Saccharomyces cerevisiae*), Sup35p (*Saccharomyces cerevisiae*), Rnq1p (*Saccharomyces cerevisiae*), HET-s

(*Podospora anserina*) and neuron-specific isoform of CPBE (*Aplisia californica*) (Chiti and Dobson, 2006).

1.4. Amyloid aggregate forming proteins

Amyloid formation may be an intrinsic property of most proteins and not just of those involved in disease states (Polverino de Laureto et al., 2003). The SH3 domain which is found in many proteins was shown to rapidly form amyloid fibrils thus initiating the hypothesis that probably the capability to form amyloid is more widespread among proteins. Thus in addition to the disease associated amyloid forming proteins (for e.g. Huntingtin, Alpha-synuclein, A β peptide and Lysozyme etc) several non-disease associated amyloid-forming proteins (e.g. BSA, HSA, Sup35 and Curlin etc) have been identified and studied. Non-disease amyloid forming proteins have been used as a model system to understand: 1. General mechanism of formation of amyloid (Bhattacharya et al., 2011). 2. Amyloid cross-seeding e.g. study of crossing of species barrier by : (a) sup35 prion protein between *S. cerevisiae* and *C. albicans* (Vishveshwara and Liebman, 2009). (b) cow prions are infectious to humans causing vCJD disease (Zou and Gambetti, 2009). 3. Potential application as structural nano-materials (Cherny and Gazit, 2008); 4. The propagation of amyloid and prion e.g. sup 35 is used to study the infection mechanism of prion (Tanaka et al., 2005) 5. Potential application as drug delivery agent; eg. Insulin amyloid aggregates as potential sustained insulin delivery tool for diabetes treatment (Gupta et al., 2010).

1.4.1. BSA and HSA: Model amyloid aggregate forming proteins Serum Albumin

Serum albumin is a globular protein and most abundant protein in blood plasma and it is present in the all mammals at a high concentration of 5g/100ml in blood. It transports important nutrients to the cells and also isolates toxins from the cells. It serves as a carrier protein for a variety of compound, like fatty acids, amino acids, bile salts, metals, hormones, drugs and pharmaceuticals. It is also responsible for the maintenance of blood pH and osmotic pressure. Serum albumin is synthesized by the liver initially as a preproalbumin. Subsequently, removal of the signal peptide makes proalbumin which is further processed by the removal of six-residue propeptide from the new N-terminus. Then the albumin is released into circulation which possesses a half-life of about 19 days (Holm et al., 2007).

Bovine Serum Albumin (BSA) and Human Serum Albumin (HSA)

BSA is the serum albumin found in a biological subfamily Bovinae (domestic cattle, African buffalo, the water buffalo, the yak, and the four-horned antelopes etc) and HSA is the serum albumin present in human blood. These proteins are acidic, all alpha structured, highly soluble, multi-domain and also show high structural stability. The Molecular weight of BSA and HSA are 66 KD and 67 KD respectively. Both BSA and HSA are made of a single peptide chain of 583 and 585 amino acids respectively with one free sulfhydryl group (on Cysteine 34) and 17 intrachain disulfide bonds (Taguchi et al., 2012). The secondary structures of BSA and HSA molecules are composed of ~ 67% alpha-helix, no beta-sheet, 10% turn, and 23% extended chains. The 3-D structure of BSA is very similar to the HSA, because the two proteins share over 76% sequence identity (Huang et al., 2004). The heart-shaped serum albumin molecule consists of three homologous-helical domains (I, II, III). Each domain contains two subdomains (A and B) that share common structural motif (**Figure 7**). Each domain can be divided into 10 helical segments: for example, h1–h6 for the subdomain A and h7–h10 for the subdomain B (Satyajit Patra et al., 2012) (Sugio et al., 1999). However, HSA contains one tryptophan residue (Trp 214) as opposed to two Trp residues in (Trp 135 and Trp 214) BSA (Gelamo and Tabak, 2000).

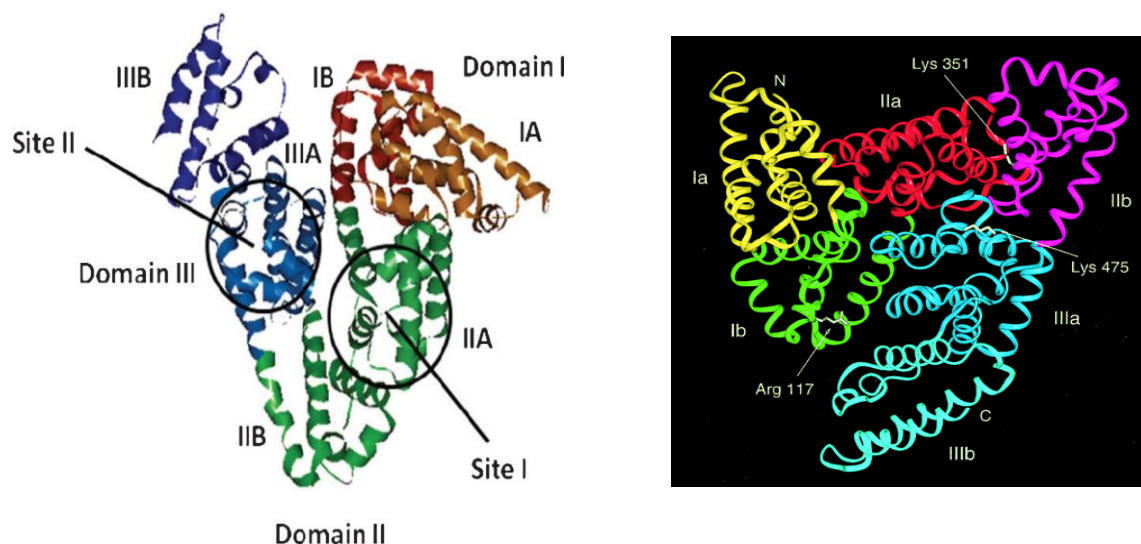


Figure 7: (a) A BSA model structure from homology modelling (Satyajit Patra et al., 2012). **(b) Crystal structure of the HSA molecule.** Each subdomain is marked with a different color (yellow for subdomain IA; green, Ibo; red, IIa; magenta, Ibis; blue, IIac; and cyan, Jib). N- and C-termini are marked as N and C, respectively. Arg117, Lys351 and Lys475, which may be binding sites for long-chain fatty acids, are colored white (Sugio et al., 1999).

1.4.2 BSA and HSA form amyloid aggregates

BSA and HSA molecules have been shown to form aggregates at elevated temperatures. Previous studies have confirmed that these thermal protein aggregates have amyloid properties (Militello et al., 2004) (Vetri et al., 2011). To confirm their amyloid nature Th-T dye binding assay, Congo red dye binding assay, electron microscopy and atomic force microscopy (**Figure 8**) etc have been previously performed (Holm et al., 2007, Juarez et al., 2009a).

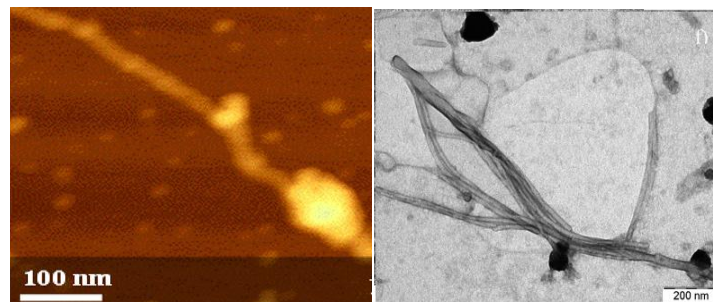


Figure 8: AFM and TEM images of BSA (Vetri et al., 2011) & HSA amyloid (Juarez et al., 2009b)

1.4.3 Aggregation pathways of serum albumins

BSA and HSA can form amyloid aggregates at low pH 3.0 (Gly-HCl buffer) or at physiological pH 7.4 (Sodium phosphate buffer) but only at high temperature, 65°C.

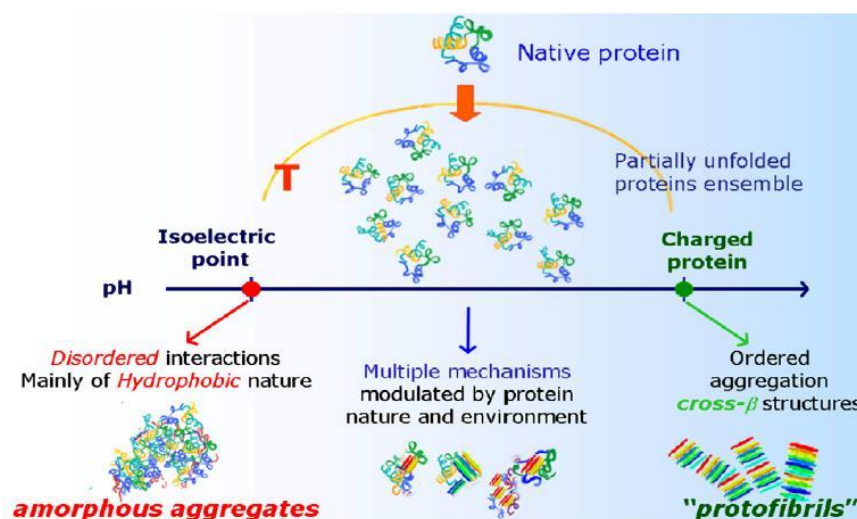


Figure 9: Sketch of BSA aggregation pathways (Vetri et al., 2011).

As shown in **figure 9**, high temperature induces partial unfolding of the protein thereby exposing the reactive areas. Further, the pH of the solution determines the type of aggregate formation. If pH is close to the isoelectric point, it leads to the formation of amorphous aggregates due to lack of

electrostatic repulsion and non-specific interaction of hydrophobic nature. At pH away from the isoelectric point, β -rich aggregates are formed as the electrostatic repulsion slow down the process thereby favouring the reorganization of aggregates into ordered form. At intermediate pH, interplay between various mechanisms may occur.

HSA has been used as a plasma expander and its administration is considered to be helpful in the treatment of severe hypoalbuminemia during burns, nephritic syndrome, chronic liver cirrhosis and haemorrhagic shock (Taguchi et al., 2012). Furthermore, the homodimer of HSA is found to more potent than monomers as a plasma expander and drug carrier. Some of the examples of shortcomings of monomers are: 1. during many pathological and physiological conditions there is increase in the capillary permeability therefore, accumulation of albumin occurs in the extravascular compartment causing oedema leading to the worsening of the disease condition. 2. In nephritic syndrome, loss of HSA monomer takes place easily due to damaged glomerulus. 3. Enhanced permeability and retention (EPR) effect of HSA monomer is less than its dimer. These shortcomings can be overcome by using HSA dimer in place of HSA monomer which has higher molecular weight. Expectedly, during increase capillary permeability, HSA dimer maintains its concentration in the blood and the loss of albumin via kidney is also reduced. And EPR effect is also increased in case of HSA dimer due to increase in molecular weight and increase uptake of albumin in the solid tumours (Taguchi et al., 2012). Since amyloid form of a HSA homodimer would have even higher molecular weight, it may possibly be an even better albumin substitute. Furthermore, even after dissolution of the amyloid, it would release dimer molecules which do not cross the vasculature as easily as the monomer HSA does. In addition, if the circulatory life of HSA conjugated with a therapeutic protein needs to be increased further, probably, using amyloid converted form of the HSA-therapeutic protein heterodimer may be of help provided it is non-cytotoxic. In the view of the above two possible applications, here we attempted to make homodimer of HSA and convert it into amyloid form.

CHAPTER II

MATERIALS AND METHODS

2.1 Materials

Bovine serum albumin (BSA) (product number A5611), Human serum albumin (HSA) (product number A6608), Congo red (CR), Thioflavin T (ThT), N-Lauroylsarcosine sodium salt (Sarkosyl), Sodium dodecyl sulphate (SDS), 5, 5'-DITHIO-BIS (2-NITROBENZOIC ACID) (Ellman's reagent) were purchased from Sigma-Aldrich. Sodium chloride, Sodium phosphate dibasic and monobasic were purchased from Himedia. All other chemicals were also of high purity.

2.2 Preparation of BSA and HSA protein amyloid aggregates

BSA and HSA proteins were dissolved in 10mM sodium phosphate buffer pH 7.4 + 50mM NaCl to a final concentration of 10-20 mg/ml and incubated at 65°C in a water bath for 6 hrs and 52 hrs respectively without agitation (Holm et al., 2007, Juarez et al., 2009a).

2.3 Confirmatory assays for Amyloid formation

2.3.1 Thioflavin T dye binding assay

First, 40µl of BSA aggregate sample was mixed with 2.6µl of ThT from a 30 mM stock solution. Th-T fluorescence emission intensity was measured in a Molecular Devices M5e Spectra Max Multimode microplate reader with excitation and emission wavelengths of 450 and 485nm respectively. Excitation spectrum was recorded by scanning the excitation wavelength from 250 nm to 470 nm and detecting emission at 495 nm. For emission spectrum, excitation wavelength was fixed at 450nm and emission was scanned from wavelength 460nm to 560nm (LeVine, 1993).

2.3.2 Congo red dye binding assay

HSA and BSA aggregates were added with Congo red dye dissolved in phosphate buffered saline, pH 7.4 in 1:1 (150µM) molar ratio and the mixture was incubated for 30 min at RT. Subsequently, absorbance spectrum was measured from 250nm to 700nm in Molecular Devices M5e Spectra Max

Multimode microplate reader (Holm et al., 2007) (Hawe et al., 2008). Increase in the absorbance value at 540 nm or generation of a shoulder peak at 540 nm was interpreted as amyloid-like successful Congo red binding.

2.3.3 Intrinsic tryptophan fluorescence

Intrinsic fluorescence of Tryptophan residues is a good parameter to study folding and unfolding of a protein (Vivian and Callis, 2001). When amyloid formation occurs, Trp residues present on the surface (hence in hydrophilic micro-environment) of the native protein may be expected to get internalized (hence in hydrophobic micro-environment) leading to change in the Trp fluorescence emission pattern. Thus, Trp fluorescence emission spectra was recorded (excitation wavelength at 292nm; emission scan 300-400nm) to study HSA/BSA amyloid formation as these molecules contain surface Trp residues in their native conformation (Wang et al., 2010).

2.3.4 Test for self-seeding of BSA /HSA amyloid aggregates

Amyloid aggregates are ordered structures and display striking ability of self-seeding whereby the pre-formed aggregates recruit the un-aggregated monomers of the same molecule and convert them also into amyloid aggregates. Amyloid seeding was monitored using Molecular Devices M5e Spectra Max Multimode microplate reader and Thioflavin T fluorescence was used to track the amyloid formation. 5% pre-formed seed was added to the monomeric protein and amyloid conversion of the monomeric protein was assayed. The excitation wavelength was set at 450nm and the emission wavelength at 485nm. The rate of aggregation was monitored for a duration of 99hrs.

2.4. Amyloid stability assays

2.4.1 Comparison of detergent stability of BSA and HSA amyloid aggregates

The analysis of molecular sizes of amyloid aggregates and their detergent insolubility was done by Semi-denaturing detergent-agarose gel electrophoresis (SDD-AGE) (Halfmann and Lindquist, 2008). Firstly, 1.5% agarose gel containing 0.1% SDS was prepared and BSA monomer (80 µg), HSA monomer (70 µg), BSA amyloid aggregates (200 µg) and HSA amyloid aggregates (240 µg) were loaded using a sample buffer containing 1% Sarkosyl in place of SDS. Samples were pre-incubated for

10 minutes at RT before electrophoresis. After electrophoresis, the samples were electro-blotted to a PVDF membrane for three hours and the membrane was subsequently stained with staining solution containing Coomassie R-250 dye. The molecular sizes of the amyloid aggregates was calculated by generating a calibration curve using relative mobility of marker proteins.

2.4.2 Comparative pH stability of BSA and HSA amyloid aggregates

BSA and HSA amyloid aggregates were equilibrated at different pH (20mM Gly-HCl buffer pH 2.0; 20mM Sodium acetate-acetic acid buffer pH 4.0; 20mM Sodium-phosphate buffer pH 6.0; 20mM Tris-HCl pH 8.0; or 20mM Glycine-sodium hydroxide pH 10.0) for determining their relative pH stabilities. Thioflavin-T was added to the samples and its fluorescence was measured to estimate the residual amyloid and hence the residual stability.

2.4.3 Comparative stability of BSA and HSA amyloid aggregates at pH6.0 and 40°C

It is known that tumour cells have low pH due to increase in production of lactic acid and high temperature due to increase in their metabolic rates. In fact, the cytotoxicity of some anti-cancerous drugs is also increased at lower pH (pH 6.0) and higher temperature (40°C) (Hahn and Shiu, 1983). Possibly, amyloid aggregates could be used to carry anti-cancerous drugs as amyloid aggregates are relatively thermo-stable (Surmacz-Chwedoruk et al., 2014) (Arora et al., 2004). Therefore, the stability of amyloid aggregates formed at pH 7.4 (normal conditions) was compared with pH 6.0 at 40°C. This was achieved by bringing down the pH of amyloid aggregates in pH 7.4 to pH 6.0 and increasing the incubation temperature to 40 °C. Then the samples were ultra-centrifuged for 35 mins at 30,000 rpm and 4°C in Beckman Coulter table top Optima™ MAX-XP ultracentrifuge. The relative distribution of the amyloid aggregates between supernatant and pellet was assessed using Thioflavin T binding assay, Bradford assay and SDS-PAGE. It would be expected that dis-aggregation of the amyloid due to lack of its stability under a given condition would increase the protein content in the supernatant fractions.

2.5. Disulphide linked conjugation using free cysteine to obtain homo-dimers of BSA/HSA

2.5.1 Estimation of free Sulphydryl group of BSA and HSA by Ellman's reagent assay

5,5'-dithiobis-(2-nitrobenzoic acid) (DTNB) also known as Ellman's reagent was used to determine the number of free sulphydryl group in HSA/BSA proteins (Ellman, 1959). Sulphydryl groups may be quantitated by using the extinction coefficient of TNB released upon reaction with DTNB. Protein samples of BSA, HSA or lysozyme at 0.15mM concentration were mixed with DTNB (4mg/ml) in the reaction buffer (sodium phosphate buffer pH 8.0) and incubated for 15 minutes at RT and absorption was measured at 412nm. Subsequently, free -SH group content was calculated using the following equation. The reported molar absorptivity of TNB in this buffer system at 412nm is 14,150. Molar absorptivity, E , is defined as follows:

$$E=A/bc \text{ (where, } A = \text{absorbance, } b = \text{path length in cm, } c = \text{concentration in moles/liter)}$$

Solving for concentration gives the following formula: $c=A/bE$.

2.5.2 Induced disulphide linked dimerization of BSA and HSA using H₂O₂

Hydrogen peroxide was used as an oxidising agent for the dimerization of the BSA and HSA and the formation of dimers was confirmed by SDS-PAGE. A final concentration of 25mM H₂O₂ was used for the oxidation reaction of 150 μM BSA (or 150μM HSA) to induce the formation of the disulphide bonds. The reaction was performed in 8M urea to ensure the accessibility of -SH group of the cysteine residues as they are located in ~10 Å deep crevice (hydrophobic pocket) in the native BSA/HSA molecules (Francis, 2010).

2.5.3 Purification of the homo-dimers of HSA/BSA by size exclusion chromatography

As the H₂O₂ induced dimerization of both BSA and HSA was not 100% therefore, the dimers needed to be separated from the monomers for analysis of their amyloid formation ability. Using gel column chromatography (Superose 6, 10/300 GL and exclusion limit is 4×10^7), FPLC (ÄKTA™ FPLC™) system was performed to separate the dimes from the monomers which differ by ~ 66 kDa molecular weight. Monomers and dimers were present in a 50mM Gly-HCL + 150mM NaCl buffer pH 3.0 (loading buffer) and 50mM Gly-HCL + 150mM NaCl buffer pH 3.0 was used for equilibration and elution. Briefly, 400μl of HSA conjugation reaction mixture containing 20 mg/ml of HSA proteins was

dialysed to remove the H₂O₂. After dialysis, the concentration of HSA was found to be 10 mg/ml and this mixture was loaded on to the SEC column for separation of the monomers and dimers. The elution of the proteins was monitored by absorption at 280 nm and fractions of 1ml and 250µl volume were collected in case of BSA and HSA respectively. The fractions containing protein were analysed by SDS-PAGE to detect the presence of monomer or dimer molecules. Those fractions containing dimers were pooled together and further used for amyloid formation. SEC purification of BSA dimers was also performed following the method described above for HSA dimer purification.

CHAPTER III

RESULTS AND DISCUSSION

3.1 *In vitro* formation of BSA and HSA protein amyloid aggregates

BSA and HSA proteins were dissolved in 10mM sodium phosphate buffer pH 7.4 containing 50mM NaCl at a concentration of 20 mg/ml. Fibrillization was induced by incubation without shaking at 65°C for 6 hrs for BSA and 52 hrs for HSA. Subsequently, confirmatory assays were performed as described below, to assess the formation of amyloid aggregates.

3.2 Confirmatory assays of BSA and HSA amyloid aggregation

3.2.1 BSA and HSA amyloid aggregation detected by Thioflavin T dye binding Assay:

Increase in ThT emission fluorescence intensity at 485 nm when excited at 450 nm usually occurs when ThT binds to amyloid aggregates. After incubation under fibrillization conditions, the ThT fluorescence emission intensity for BSA and HSA amyloid aggregates showed over 19 fold and 11 fold increase respectively (**Tables 2 & 3**). This strongly suggests that BSA and HSA proteins have undergone amyloid conversion.

Table 2: Thioflavin-T fluorescence intensity (AU) at 485 nm for BSA

Blank (pH 7.4 buffer)	BSA amyloid aggregates	Fold increase
148.7	2943.8	19.7

Table 3: Thioflavin-T fluorescence intensity (AU) at 485 nm for HSA

Blank (pH 7.4 buffer)	HSA amyloid aggregates	Fold increase
226.6	2575.7	11.3

ThT Excitation and Emission spectra for BSA and HSA fibrillization: ThT free dye normally shows excitation maximum at 385 nm and emission maximum at 445 (LeVine, 1993). However, when Th-T binds with amyloid aggregates, it shows fluorescence excitation maximum at 450 nm

and emission maximum at 445nm. The obtained BSA aggregates showed ThT excitation maximum λ_{max} at 444 nm and emission maximum λ_{max} at 494 nm whereas the HSA aggregates showed excitation maximum λ_{max} at 450 and emission maximum λ_{max} at 496 nm (**Figures 10 & 11**). These observations strongly indicate amyloid nature of the aggregated BSA and HSA proteins.

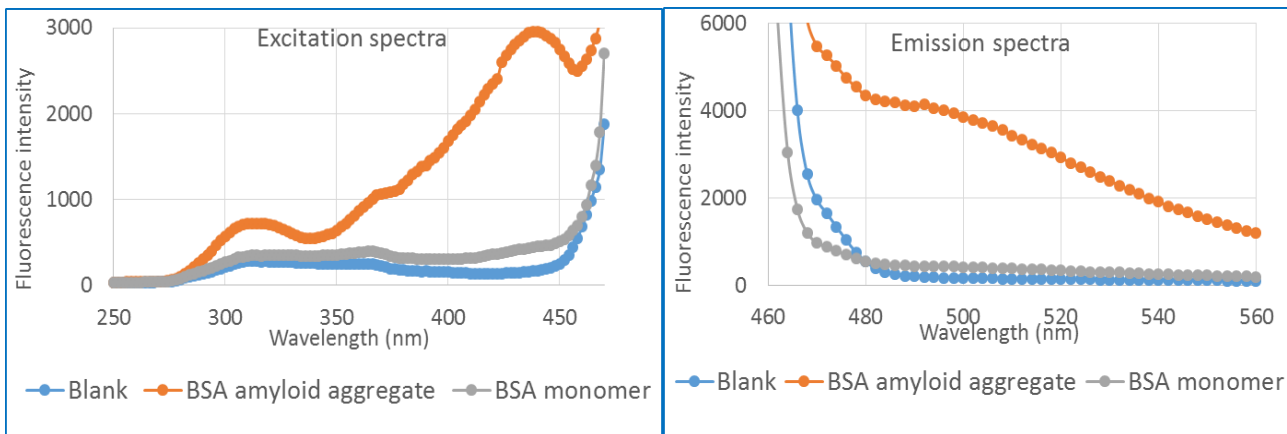


Figure 10: ThT Excitation and Emission spectra for BSA fibrillization

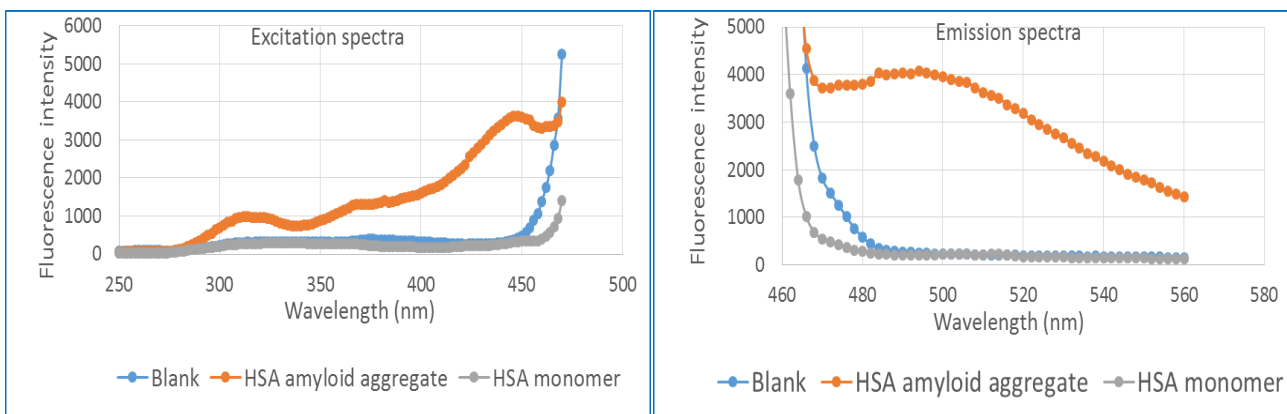


Figure 11: ThT Excitation and Emission spectra for HSA fibrillization

3.2.2. BSA and HSA amyloid aggregation detected by Congo-Red dye (CR) binding Assay:

When CR binds with amyloids its absorption spectrum shows red-shift in its absorption maximum (from around 490 to 540 nm) and higher absorption intensity at 540 nm (Hawe et al., 2008). The CR+BSA and CR+HSA aggregates obtained here, exhibited red shift from 490 to 540 nm and higher absorption near 540nm as compared with unbound CR spectrum (**Figure 12**). These results are consistent with the presence of amyloid-like nature of the obtained BSA and HSA aggregates.

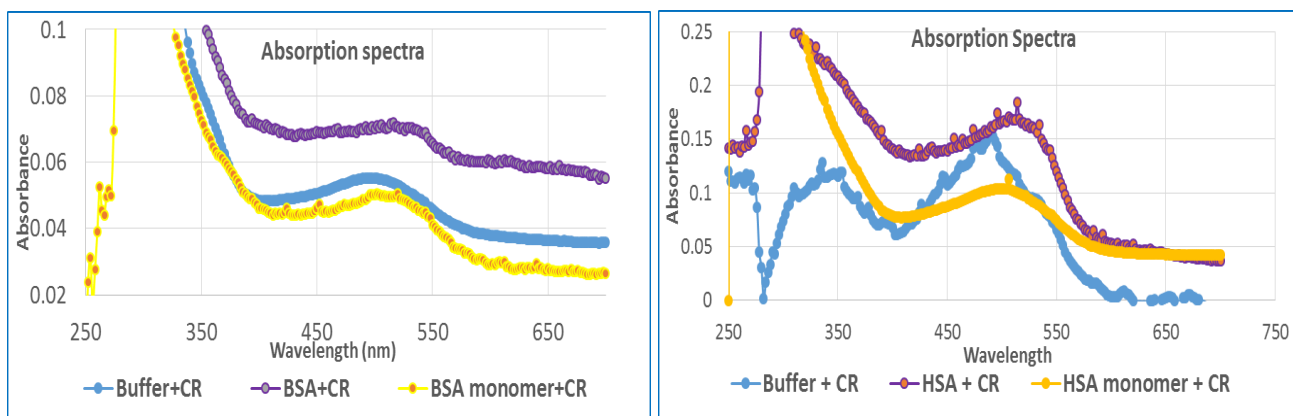


Figure 12: CR absorption spectra for BSA and HSA fibrillization

3.2.3. Intrinsic Tryptophan fluorescence of BSA and HSA amyloid aggregates:

The BSA and HSA aggregates obtained here showed intrinsic Trp emission maxima λ_{max} at 334nm and 332nm as compared with their un-aggregated monomeric BSA and HSA emission maxima λ_{max} of 342nm and 340nm respectively (**Figure 13**). The observed blue shift of ~ 8 nm in the emission maxima are indicative of movement of tryptophan residues to relatively hydrophobic micro environment in both BSA and HSA aggregates (**Table 4**). This data is consistent with an expected internalization of any surface Trp residues during amyloid aggregate formation.

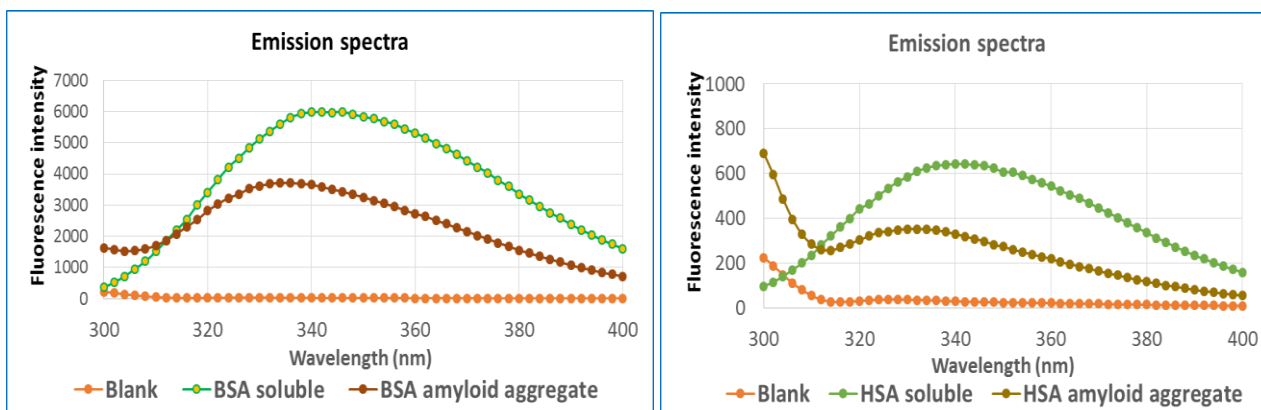


Figure 13: Intrinsic Tryptophan fluorescence of BSA and HSA amyloid aggregates.

Table 4: Emission maxima (λ_{\max}) of BSA and HSA monomers vs amyloid aggregates

	BSA		HSA	
	Monomer	Amyloid aggregate	Monomer	Amyloid aggregate
λ_{\max}	342 nm	334 nm	340 nm	332nm

3.2.4. Assay of self-seeding nature of BSA & HSA amyloid aggregates:

The ability to self-seed the aggregation of their monomers under optimal conditions distinguishes the amyloid aggregates from amorphous aggregates. However, under experimental conditions, to visualize the process of seeding, a lag dependent growth of the amyloid is pre-requisite. Any reduction in the lag period upon addition of the pre-formed seed is interpreted as successful seeding. Previously, it is shown that BSA and HSA amyloid aggregate formation proceeds without any lag phase at 65°C fibrillization temperature (Holm et al., 2007). Therefore, self-seeding ability of pre-formed BSA or HSA aggregates could not be monitored at optimal 65°C fibrillization temperature. Therefore, we examined a suboptimal fibrillization temperature (40°C) where spontaneous aggregation would be negative due to lack of successful oligomeric nuclei formation which normally precedes the amyloid aggregates. However, the added pre-formed seed which contains pre-formed nuclei may initiate the conversion of the monomers to aggregates and show the seeding kinetics even at suboptimal temperatures. Indeed, as per our hypothesis, the BSA amyloid aggregates did show self-seeding even at 40°C as observed by increase in ThT fluorescence increase and shape of the emission spectrum (**Figures 14 & 15**). However, under these conditions the HSA aggregates did not exhibit self-seeding thereby suggesting of differences between the amyloid growth energetics of BSA and HSA proteins (**Figures 14 & 15**).

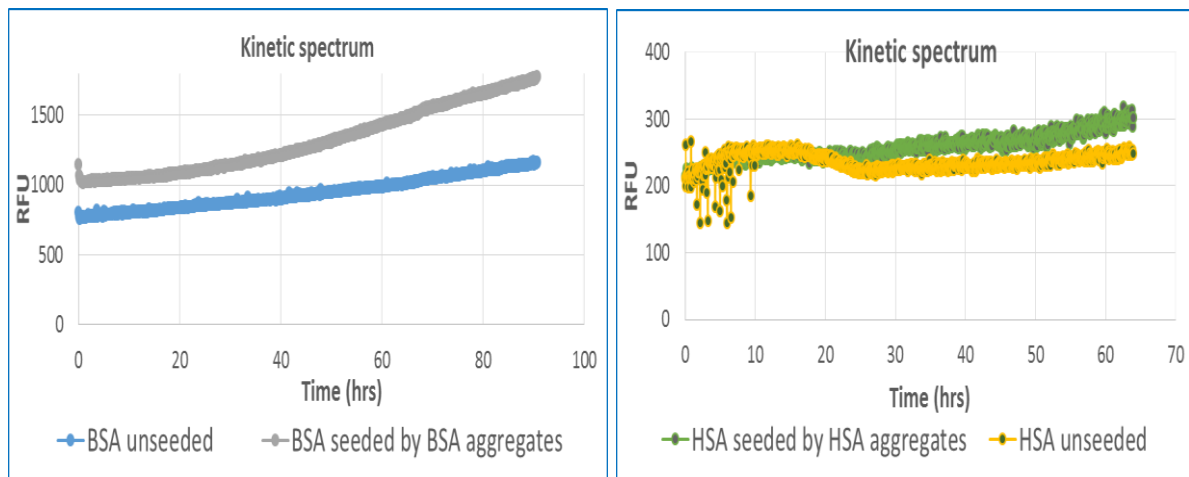


Figure 14: Assay of self-seeding kinetics for BSA and HSA aggregation at suboptimal temperature (40°C).

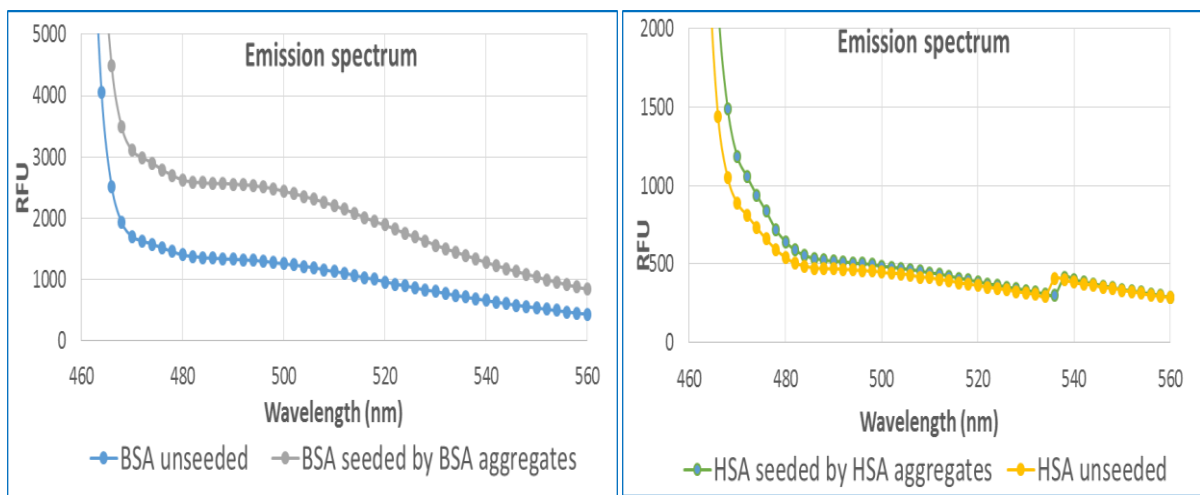
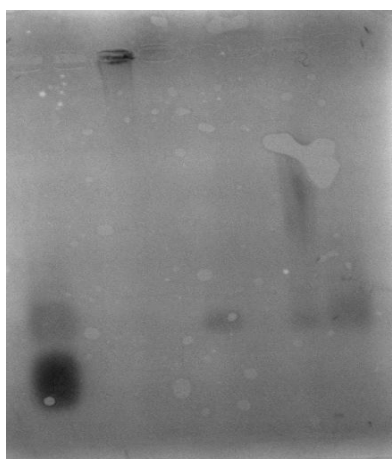


Figure 15: Assay of amyloid-like emission spectra of BSA and HSA samples after self-seeding kinetics shown in figure 14.

3.3 Comparative stability of BSA and HSA amyloid aggregates

3.3.1 Detergent stability by Semi-denaturing detergent agarose gel electrophoresis:

Protein amyloid aggregates show increased stability against denaturants (eg. Urea) and ionic detergents (eg. SDS & sodium lauroyl sarcosinate i.e. Sarkosyl) when compared with amorphous aggregates. To compare the stabilities of the BSA and HSA amyloid aggregates, we investigated their resistance to 1% sarkosyl at room temperature using SDD-AGE. As shown in **Figure 16**, both the HSA and BSA aggregates exhibited higher molecular weight species even after sarkosyl treatment indicating their resistance against dis-aggregation of sarkosyl.



1.5 % Agarose gel

Left to Right

Lane 1 – Lysozyme + BSA monomer

Lane 2 - HSA aggregate (240µg)

Lane 3 - HSA monomer (70µg)

Lane 4 – BSA aggregate (200µg)

Lane 5 – BSA monomer (80µg)

Figure 16: SDD-AGE analysis of HSA and BSA aggregates

Whereas, the BSA amyloid aggregate showed large smear much above the band of its monomer, the HSA amyloid aggregate failed even to enter the gel indicating a very large size. Thus, HSA and BSA amyloid aggregates differ significantly with regards to the sizes of their sarkosyl stable species. Using calibration curve generated by relative mobility of known proteins, it was estimated that the sarkosyl-stable species of BSA and HSA amyloid aggregates were about 995 kDa and 6084 kDa size and composed of about 15 and 90 monomers respectively (**Tables 5 & 6**). In addition, this observed sarkosyl stability strongly supports amyloid nature of these BSA & HSA aggregates.

Table 5. Relative mobility of molecular weight markers on SDD-AGE

	Molecular Weight (kDa)	Distance moved (cm)	Gel front (cm)	Relative mobility
BSA soluble	66	4.7	7.1	0.661
HSA soluble	67	4.5	7.1	0.633
Lysozyme	14	6.1	7.1	0.859

Table 6. Estimated mol. wt. of sarkosyl-stable BSA and HSA amyloid aggregate species

	Distance moved (cm)	Gel front (cm)	Relative mobility	Calculated molecular Weight (kDa)	Calculated no. of monomers associated
BSA aggregate	2.1	7.1	0.295	995.47	15
HSA aggregate	0.4	7.1	0.056	6084.29	90

3.3.2 The stability of BSA and HSA amyloid aggregates at different pH: The pH stability of BSA and HSA amyloid aggregates was assayed by ThT fluorescence to check if there are any differences in their behaviour. At the fibrillization pH 7.4 where the aggregates were formed, BSA and HSA amyloid aggregates displayed 33.5 and 7.2 fold ThT fluorescence increase respectively (**Table 7 & 8**). When the raw data (**Tables 7 & 8; and Figures 17a & 17b**), were carefully analysed, we observed that the effect of pH on BSA & HSA amyloid dis-aggregation was similar on all pH values except for pH 6.0 & 8.0 (**Table 9**). At pH 6.0 and 8.0, the BSA amyloid aggregates were found to be over 16-20% more stable than HSA amyloid aggregates as seen by retention of higher ThT fluorescence (**Table 9**).

Table 7: ThT fluorescence emission intensity (AU) at 485 nm for BSA amyloid aggregates incubated at different pH

pH	Blank (Buffer)	BSA aggregates	Fold increase
pH 2.0	174	1736.6	9.9
pH 4.0	174	2237.0	12.8
pH 6.0	174	2573.7	14.7
pH 8.0	174	4789.6	27.5
pH 9.0	174	3384.4	19.4
pH 10.0	174	2838.7	16.3
pH 7.4	174	5844.1	33.5

Table 8. ThT fluorescence emission intensity (AU) at 485 nm for HSA amyloid aggregates incubated at different pH

pH	Blank (Buffer)	HSA aggregates	Fold increase
pH 2.0	224.7	519.8	2.3
pH 4.0	224.7	646.0	2.8
pH 6.0	224.7	603.4	2.6
pH 8.0	224.7	1069.9	4.7
pH 9.0	224.7	1041.1	4.6
pH 10.0	224.7	843.7	3.7
pH 7.4	224.7	1613.8	7.2

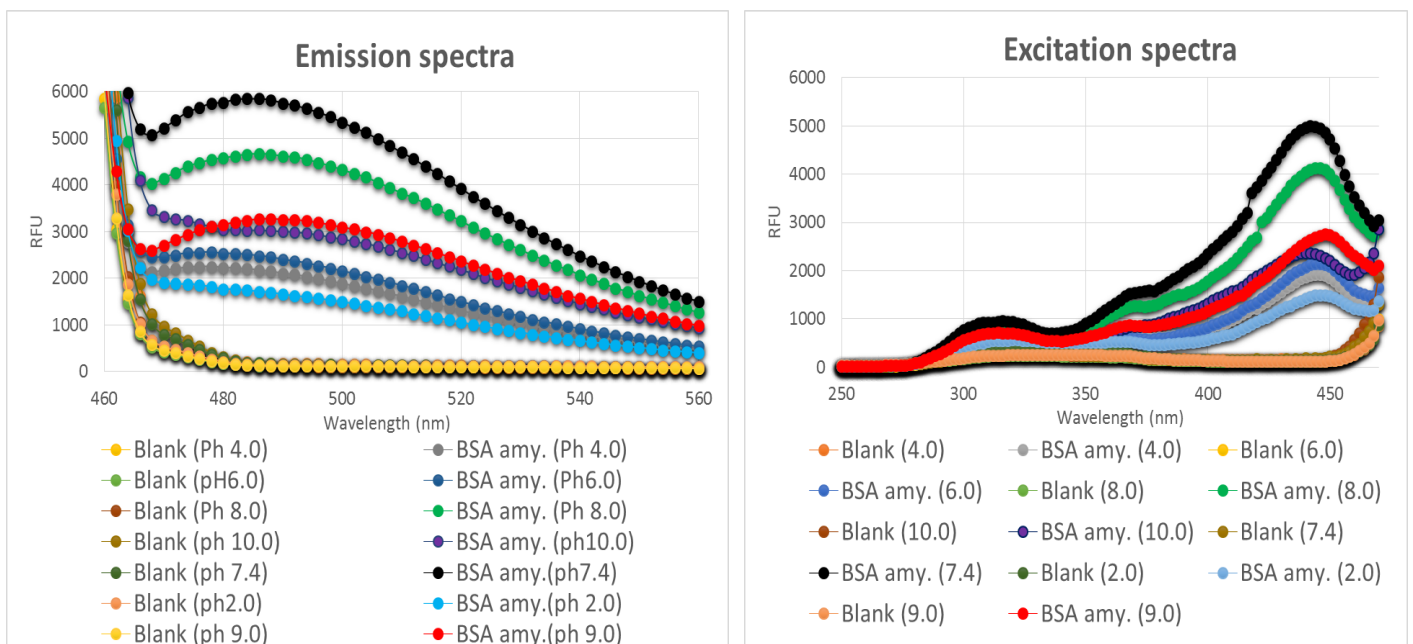


Figure 17. (a) ThT Emission and Excitation spectra of BSA amyloid aggregates at different pH.

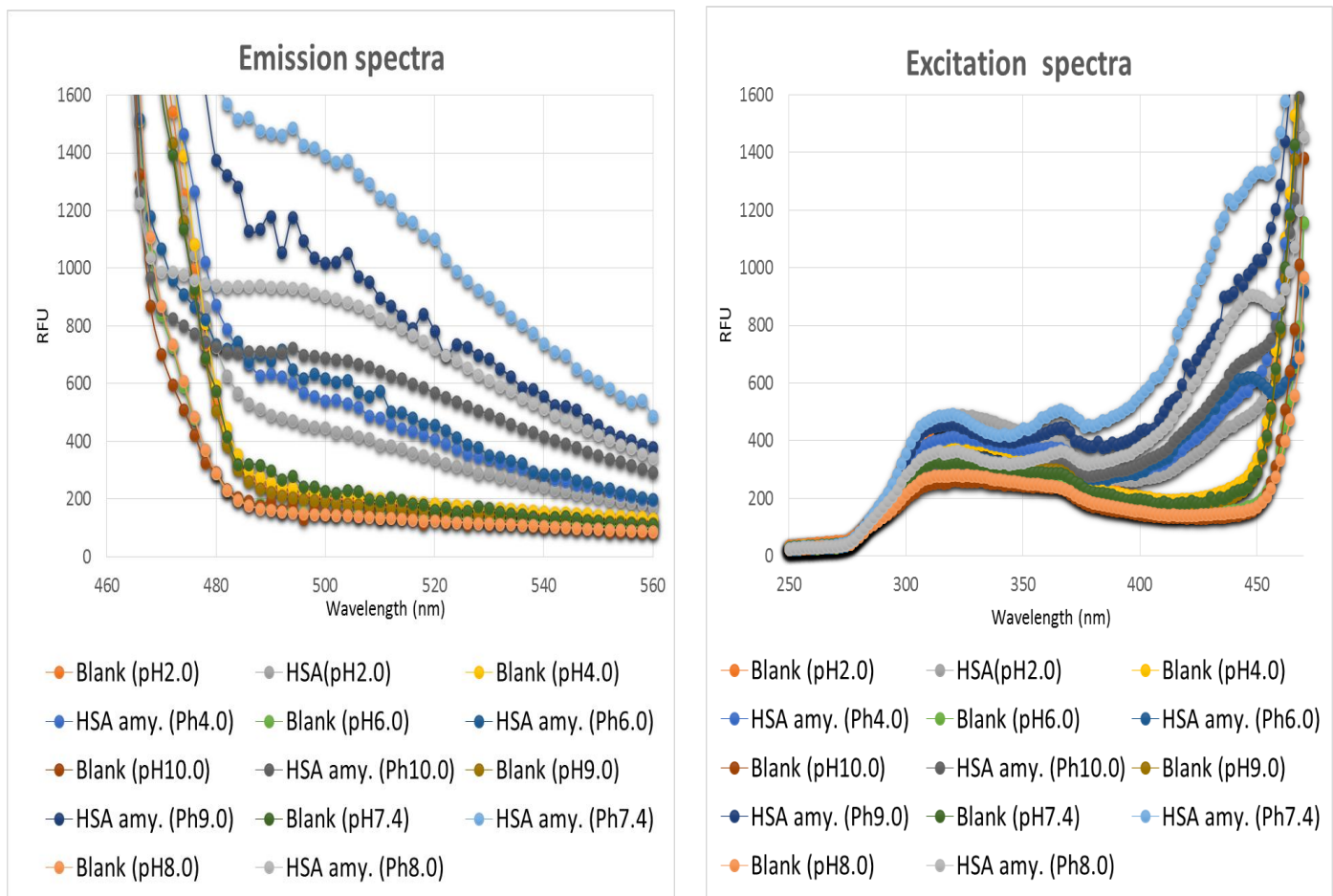


Figure 17. (b) ThT Emission and Excitation spectra of HSA amyloid aggregates at different pH.

Table 9: Comparative pH stabilities of BSA and HSA amyloid aggregates

pH	Residual ThT fluorescence of BSA (%)	Residual ThT fluorescence of HSA (%)
7.4	100%	100%
2.0	27.5%	21.2%
4.0	36.3%	33.3%
6.0	43.3%	27.2%
8.0	81.4%	60.8%
9.0	56.6%	58.7%
10.0	46.9%	44.5%

3.3.3 Comparative stabilities of BSA and HSA amyloid aggregates at pH 6.0 and 40°C:

The pre-formed aggregates of BSA & HSA at pH 7.4 were incubated at pH 6.0 at 40 °C and their stability under these conditions was assessed by ThT fluorescence. Following the incubation, amyloid aggregates were ultra-centrifuged at 40,100 x g at 4°C for 35 mins and level of ThT fluorescence was measured in the supernatant versus the pellet (The pellet was first re-suspended in the same volume of fresh pH 6.0 buffer). Furthermore, estimation of protein concentration by Bradford reagent and SDS-PAGE were also used to examine the level of protein precipitation by ultracentrifugation. It would be expected that if the amyloid is not fully stable under a condition it would dis-aggregate and partition more into the supernatant fractions after ultra-centrifugation. Alternatively, if the aggregates become larger more amyloid would be expected to partition into the pellet fractions. Indeed, by all the examined parameters [eg. ThT fluorescence (**Table 10, 11, & 12, and Figures 18 & 19**), Bradford assay (**Table 13 & 14**) or SDS-PAGE (**Figure 20**)], it was evident that both BSA and HSA amyloid aggregates increase in size when transferred from pH 7.4 to pH 6.0. But the extent of size increase is more in BSA than HSA amyloid aggregates.

Table 10. ThT Fluorescence intensity of BSA aggregates (pH 6.0, 40°C) after ultra-centrifugation

	Blank	Protein	Fold increase
pH7.4 Supernatant	204.5	5802.3	28.3
pH7.4 Pellet	204.5	434.1	2.1
pH6.0 Supernatant	149.4	2429.5	16.2
pH6.0 Pellet	149.4	988.7	6.6

Table 11. ThT Fluorescence intensity of HSA aggregates (pH 6.0, 40°C) after ultra-centrifugation

	Blank	Protein	Fold increase
pH7.4 Supernatant	217.6	491.1	2.2
pH7.4 Pellet	217.6	806.2	3.7
pH6.0 Supernatant	156.0	261.8	1.6
pH6.0 Pellet	156.0	556.6	3.5

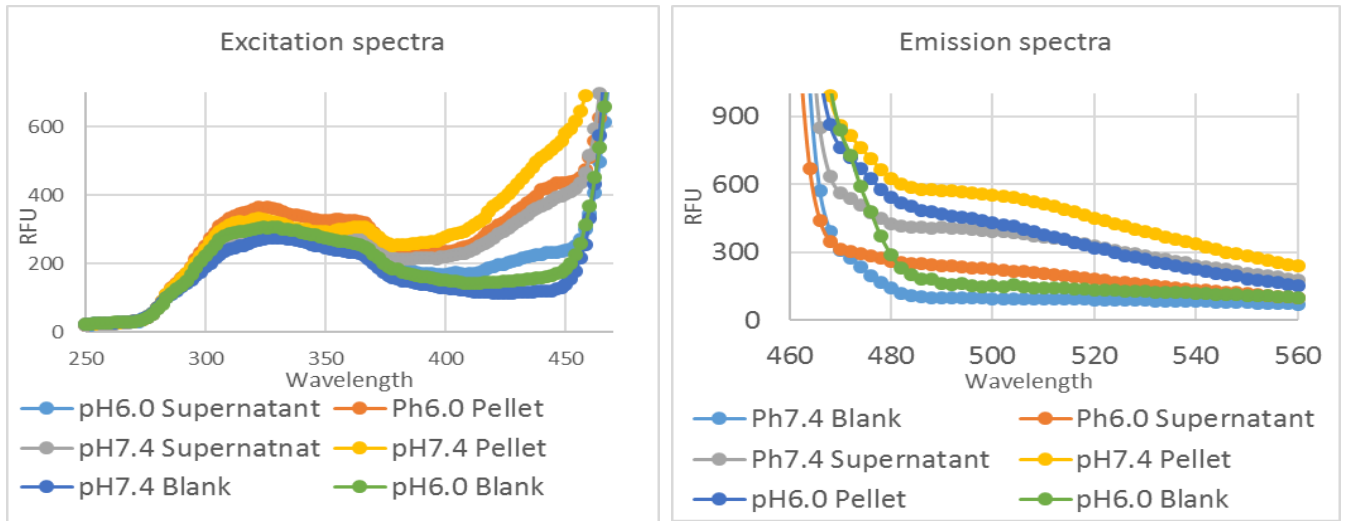


Figure 18. Residual emission and excitation spectra of BSA aggregates after incubation at pH 6.0 & 40°C

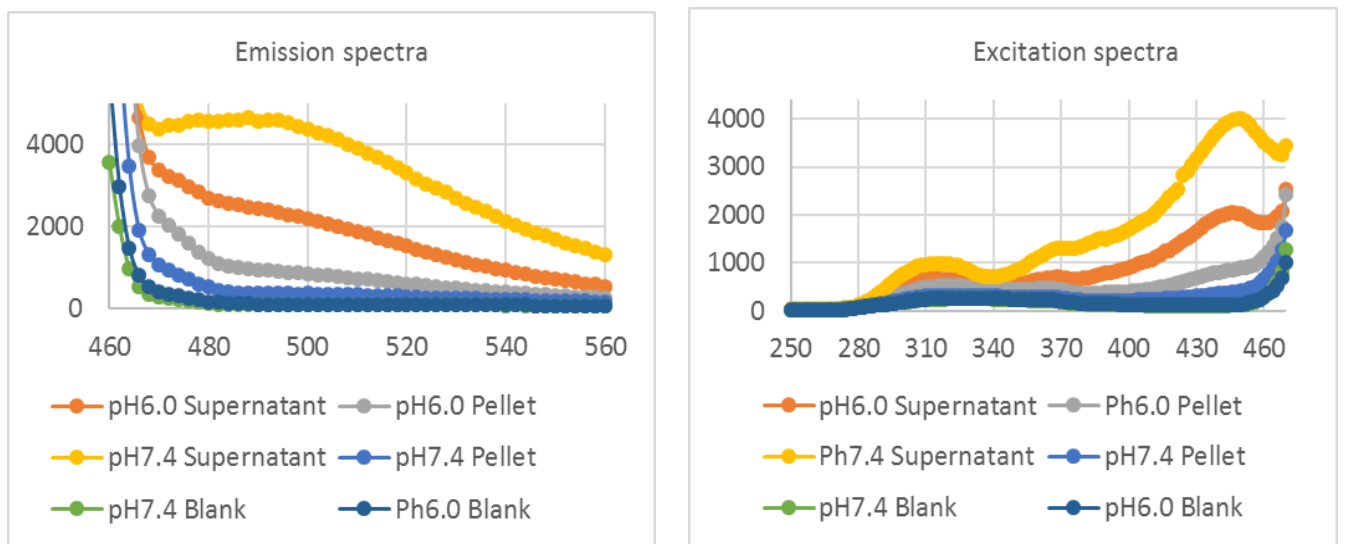


Figure 19. Residual emission and excitation spectra of HSA aggregates after incubation at pH 6.0 & 40°C

Table 12. Residual Th-T fluorescence (%) of BSA and HSA amyloid aggregates after ultra-centrifugation

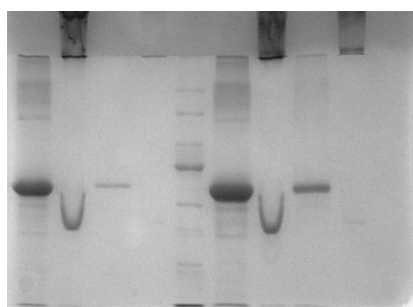
pH	BSA ThT fluorescence		HSA ThT fluorescence	
	Supernatant	Pellet	Supernatant	Pellet
7.4	96%	4%	32%	68%
6.0 & 40°C	73%	27%	21%	79%

In addition to the increase in ThT fluorescence in the pellet fractions, when shifted from pH 7.4 to pH 6.0, concomitant increase in relative protein content was also observed in the pellet fractions in both HSA and BSA amyloid aggregates (**Table 13**).

Table 13. Relative fractionation of the HSA/BSA aggregates into pellet or supernatant assayed by Bradford assay

Sample	Pellet/Supernatant at pH 7.4	Pellet/Supernatant at pH6.0
BSA amyloid aggregates	0.4	0.6
HSA amyloid aggregates	1.5	3.8

1 2 3 4 5 6 7 8 9 10



7.5% gel

Left to Right

Lane 1, 2- Supernatant pH 7.4 (R and NR)

Lane 3, 4- Pellet pH 7.4 (R and NR)

Lane 5- Marker

Lane 6, 7- Supernatant pH 6.0 (R and NR)

Lane 8, 9- Pellet pH6.0 (R and NR)

Figure 20: SDS-PAGE of BSA amyloid aggregate of supernatant and pellet at pH7.4 and pH6.0

3.4. Conjugation using free cysteine to obtain homo-dimer of BSA and HSA and examination of amyloid formation by the dimer molecules.

3.4.1 Determination of number of free cysteine by Ellman's reagent assay:

In order to dimerize the BSA or HSA molecules via disulphide linkage, the availability of the one free cysteine residue needed to be confirmed. This estimation of the free cysteine was carried out using Ellman's reagent assay using B-mercaptoethanol and Lysozyme (which has no free cysteine) as a positive and negative controls respectively (**Table 14**). BSA and HSA exhibited 1.1 and 0.50 free

sulfhydryl group per molecule respectively thus these proteins could be used for conjugation via disulphide bond formation.

Table 14. Estimation of number of free sulfhydryl groups per protein molecule

Concentration of the sample	Estimated no. of free sulphhydryl group/mol.	Published no. of free – SH group
β - mercaptoethanol (0.25 mM)	1.1	1.0
HSA (0.10 mM)	1.01	1.0
BSA (0.15 mM)	0.50	1.0
Lysozyme (0.07 mM)	0.15	0.0

3.4.2 Disulphide linked homo-dimerization of BSA and HSA: For the conjugation, a reaction mixture containing 8M urea, 25mM/100mM Hydrogen peroxide, 0.15mM BSA/HSA was prepared in reaction buffer (50mM Gly-HCL + 50mM NaCl). The 8M urea was used for exposing out the one free cysteine which is present in the 10 Å deep crevice. Hydrogen peroxide was used for the oxidation of disulphide bonds. In **figure 21**, lane 1 and 3 showed BSA dimer bands however, the ratio of dimer to monomer was ~ 1:4 showing that dimerization was an inefficient process. Also, increasing the H₂O₂ concentration from 25 mM to even 100 mM did not increase the level of dimer formation. In **figure 22**, lane 4 and 6 showed HSA dimer bands and the ratio of dimer to monomer was ~ 2:3. The only very minute levels of dimer seen in lanes 2 & 8 show that both urea and H₂O₂ together are required for efficient dimerization.

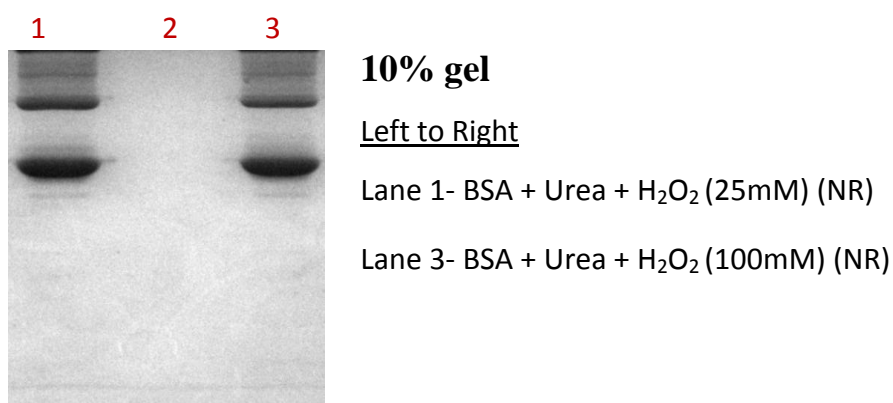


Figure 21: H₂O₂ induced dimerization of BSA examined by SDS-PAGE.

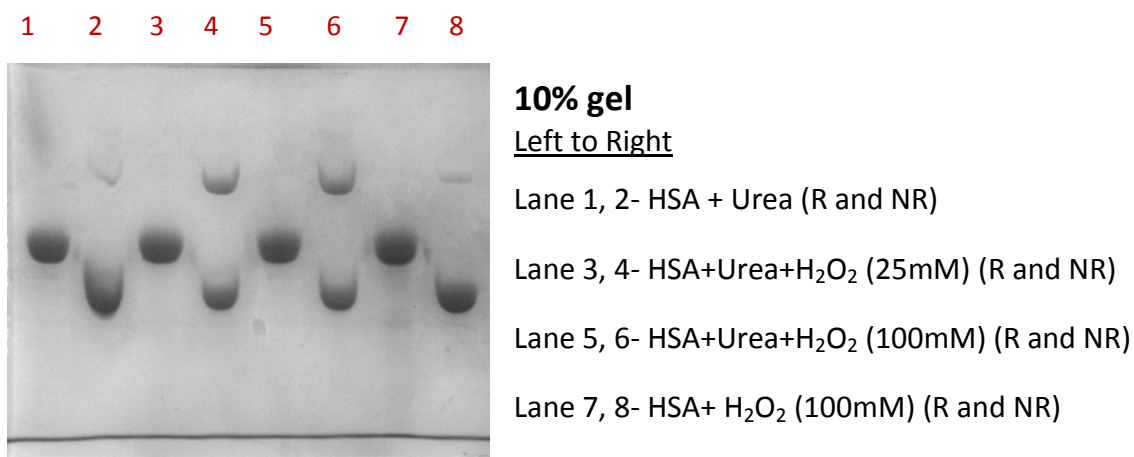


Figure 22: H₂O₂ induced dimerization of HSA examined by SDS-PAGE.

3.4.3 Purification of the homo-dimer molecules of HSA/BSA by size exclusion chromatography (SEC)

As the dimerization of HSA/BSA was far less than the expected 100%, thus the dimers needed to be purified out from the monomers prior to the assay of their amyloid forming capabilities. As the monomers and dimers differ by about 66 kDa, the purification was attempted by SEC using Superose 6 column (10/300 GL and exclusion limit is 4×10^7) on FPLC (ÄKTA™FPLC™) system. Size of fractions collected were 1ml and 250µl respectively in cases of BSA and HSA. In **figure 23 (a)**, which shows elution profile for HSA, two peaks were obtained for which the **figure 23 (b)** shows estimation of purity by SDS-PAGE. As expected, the first peak fractions contained predominantly dimer molecules while the second peak fractions showed mostly monomers. As shown in **figure 24 (a & b)**, results similar to as described above for BSA were also obtained for BSA dimer purification. The fractions containing predominantly dimers for both HSA/BSA were pooled and further analysed for amyloid formation ability.

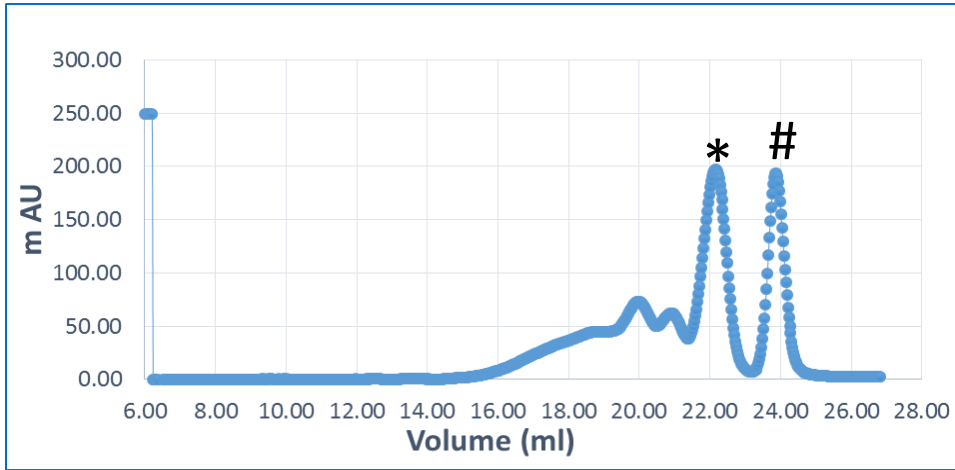


Figure 23. (a) SEC Chromatogram of HSA monomer and dimer purification

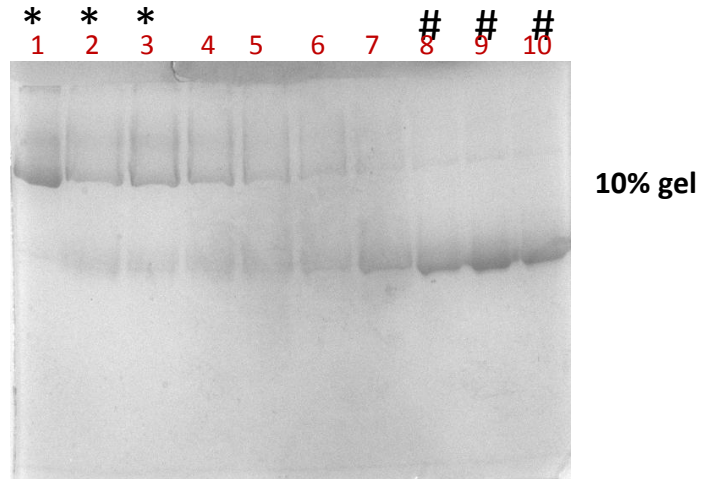


Figure 23 (b). Analysis of purity of fractions on SDS-PAGE after gel filtration from figure 23(a).

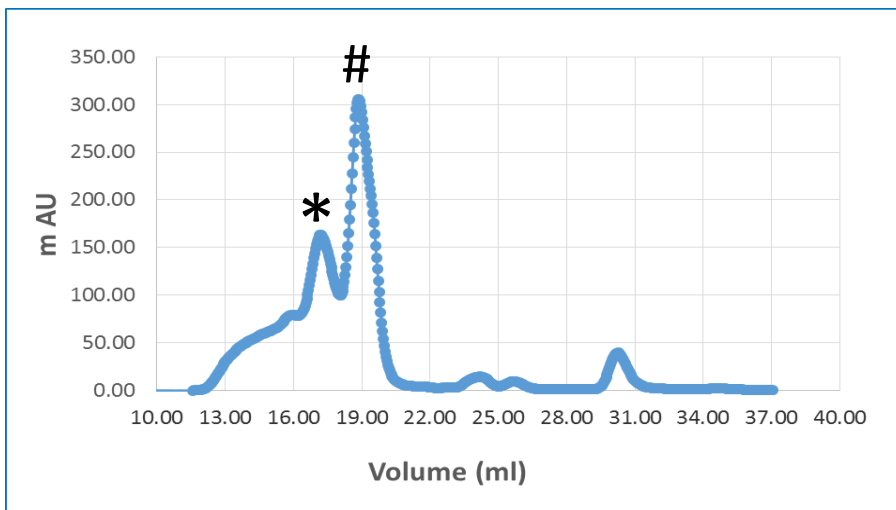


Figure 24. (a) SEC chromatogram of BSA monomer and dimer purification

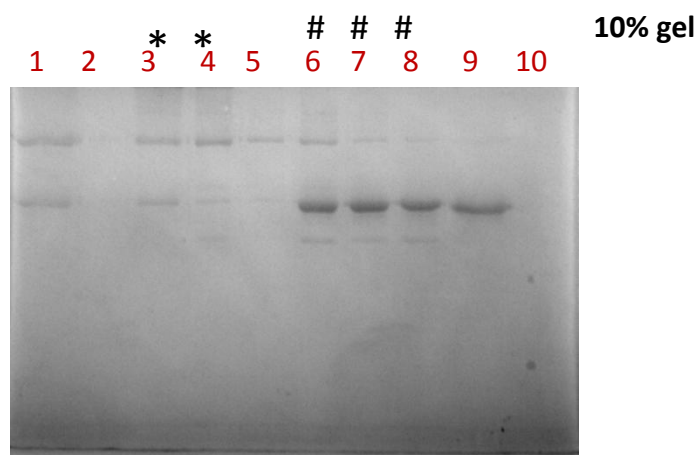


Figure 24. (b) Analysis of purity of fractions on SDS-PAGE after gel filtration from figure 24(a).

3.4.4 HSA-dimer amyloid fibrillization and its confirmatory assays

After the fractions containing HSA-dimer were obtained by SEC, ammonium sulphate precipitation was performed to increase the protein concentration. Obtained pellet was dissolved in fibrillization buffer (10mM sodium phosphate containing 50mM NaCl pH 7.4) and incubated for 52 hrs at 65°C. Following the incubation, ThT binding was examined by measuring its fluorescence emission intensity. We found that the HSA-dimer aggregates were showing over 10.8 fold increase strongly suggesting of amyloid-like nature (**Table 15**). This indicates that HSA in a dimer form have undergone amyloid conversion.

Table 15: Thioflavin-T fluorescence intensity (AU) at 485 nm for HSA-dimer

Blank (pH 7.4 buffer)	HSA-dimer amyloid	Fold increase
215.56	2334.8	10.8

In addition, the obtained HSA-dimer aggregates were showing ThT excitation maximum λ_{\max} at 440 nm and emission maximum λ_{\max} at 496 nm, consistent with as expected upon binding of ThT to amyloid aggregates (**Figures 25**).

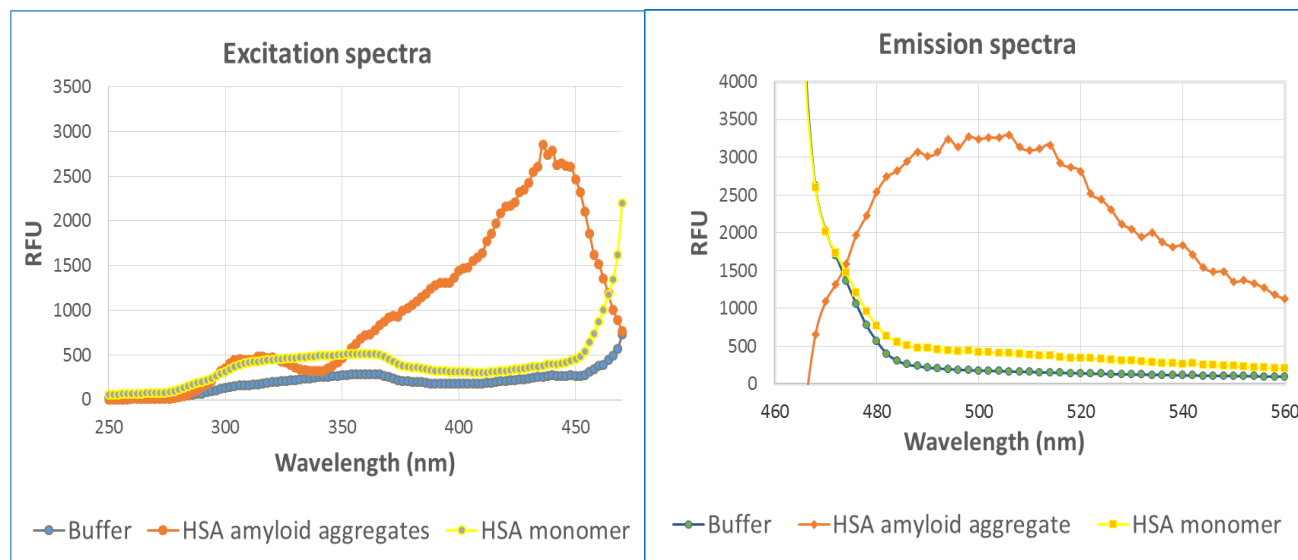


Figure 25: ThT Excitation and Emission spectrum of HSA-dimer fibrillization

Furthermore, we checked whether these HSA dimer aggregates bind to Congo red (CR). When CR binds to amyloids its absorption spectrum shows red-shift in its absorption maximum (from around 490 to 540 nm) and higher absorption intensity at 540 nm (Hawe et al., 2008). The CR+HSA dimer aggregates obtained here, exhibited red shift from 490 to 540 nm and higher absorption near 540nm as compared with unbound CR spectrum (**Figure 26**). These results are consistent with the presence of amyloid-like nature of the obtained HSA-dimer aggregates.

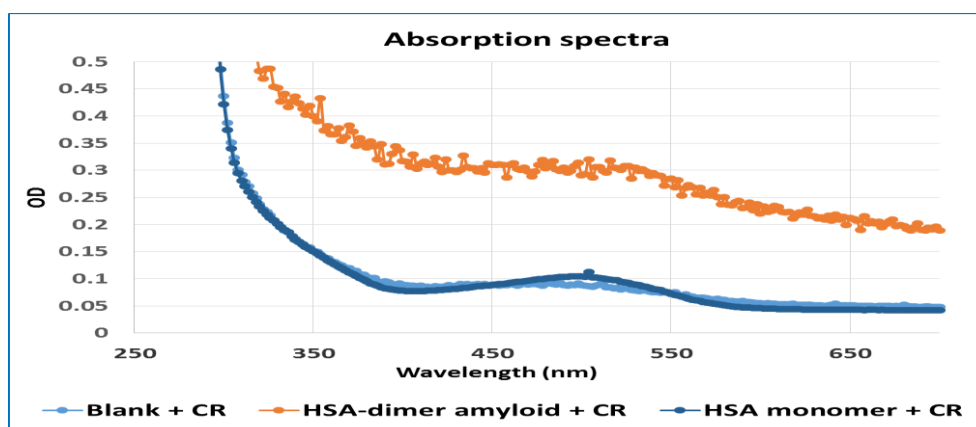


Figure 26: Absorption spectra of CR in presence of HSA-dimer aggregates.

The observed ability of HSA homo-dimer to form amyloid similar to its monomer opens the possibility that another therapeutic protein or peptide may be conjugated with HSA and hetero-dimer may be converted to amyloid form. This may find potential applications in therapeutic strategies where circulatory life of a protein/peptide needs to be increased.

CHAPTER IV

CONCLUSION

Here we succeeded in comparative analysis of properties of HSA and BSA amyloid aggregates. First, amyloid aggregates were induced to form and confirmatory assays were performed to ascertain their amyloid conformation. Interestingly, it was found that the HSA amyloid aggregates are bigger in size and more Sarkosyl detergent stable than the BSA amyloid aggregates despite the high sequence similarity between the two proteins. The BSA amyloid aggregates showed 15-20% more stability at pH 6.0 and 8.0 as compared to the HSA amyloid aggregates. At other pH values BSA and HSA amyloid aggregates were found to show similar stabilities. When shifted from the fibrillization pH 7.4 to 6.0 at 40°C, both BSA and HSA amyloid aggregates exhibited increase in the aggregate sizes. When we examined the self-seeding ability of BSA & HSA aggregates towards their monomers, a marked difference was observed between the two amyloids. Seeding ability was assayed at a suboptimal temperature (40°C) due to lack of lag period (which is pre-requisite to monitor seeding) in the fibrillization at the optimal temperature (65°C). Whereas the BSA amyloid aggregates exhibited self-seeding at the suboptimal temperature assayed, the HSA amyloid aggregates could not self-seed under the same conditions tested. This further suggests of the presence of conformational differences between the HSA and BSA amyloid aggregates.

Several therapeutic proteins have been previously conjugated to HSA in order to increase their circulatory life and hence their therapeutic duration. As the HSA amyloid aggregates are shown to be non-cytotoxic to cell cultures, we hypothesized that use of amyloid form of HSA conjugated with a therapeutic protein may further increase the circulatory life of the therapeutic protein since amyloid structures are relatively stable to clearance. As a step in this direction, and to provide proof of the principle and feasibility, we succeeded here in conjugating HSA with another HSA molecule via a disulphide linkage and further showed that indeed the dimers retains amyloid forming capabilities alike its monomers. Further studies in this direction, in future, could examine and establish the therapeutic usage of an amyloid form a HSA-therapeutic protein heterodimer.

REFERENCES

1. ARORA, A., HA, C. & PARK, C. B. 2004. Insulin amyloid fibrillation at above 100 degrees C: new insights into protein folding under extreme temperatures. *Protein Sci*, 13, 2429-36.
2. BHATTACHARYA, M., JAIN, N. & MUKHOPADHYAY, S. 2011. Insights into the mechanism of aggregation and fibril formation from bovine serum albumin. *J Phys Chem B*, 115, 4195-205.
3. CHERNY, I. & GAZIT, E. 2008. Amyloids: not only pathological agents but also ordered nanomaterials. *Angew Chem Int Ed Engl*, 47, 4062-9.
4. CHITI, F. & DOBSON, C. M. 2006. Protein misfolding, functional amyloid, and human disease. *Annu Rev Biochem*, 75, 333-66.
5. DEMURO, A., MINA, E., KAYED, R., MILTON, S. C., PARKER, I. & GLABE, C. G. 2005. Calcium dysregulation and membrane disruption as a ubiquitous neurotoxic mechanism of soluble amyloid oligomers. *J Biol Chem*, 280, 17294-300.
6. ELLMAN, G. L. 1959. Tissue sulfhydryl groups. *Arch Biochem Biophys*, 82, 70-7.
7. FRANCIS, G. L. 2010. Albumin and mammalian cell culture: implications for biotechnology applications. *Cytotechnology*, 62, 1-16.
8. GELAMO, E. L. & TABAK, M. 2000. Spectroscopic studies on the interaction of bovine (BSA) and human (HSA) serum albumins with ionic surfactants. *Spectrochim Acta A Mol Biomol Spectrosc*, 56A, 2255-71.
9. GUPTA, S., CHATTOPADHYAY, T., PAL SINGH, M. & SUROLIA, A. 2010. Supramolecular insulin assembly II for a sustained treatment of type 1 diabetes mellitus. *Proc Natl Acad Sci U S A*, 107, 13246-51.
10. HAHN, G. M. & SHIU, E. C. 1983. Effect of pH and elevated temperatures on the cytotoxicity of some chemotherapeutic agents on Chinese hamster cells in vitro. *Cancer Res*, 43, 5789-91.
11. HALFMANN, R. & LINDQUIST, S. 2008. Screening for amyloid aggregation by Semi-Denaturing Detergent-Agarose Gel Electrophoresis. *J Vis Exp*.
12. HAWE, A., SUTTER, M. & JISKOOT, W. 2008. Extrinsic fluorescent dyes as tools for protein characterization. *Pharm Res*, 25, 1487-99.

13. HOLM, N. K., JESPERSEN, S. K., THOMASSEN, L. V., WOLFF, T. Y., SEHGAL, P., THOMSEN, L. A., CHRISTIANSEN, G., ANDERSEN, C. B., KNUDSEN, A. D. & OTZEN, D. E. 2007. Aggregation and fibrillation of bovine serum albumin. *Biochim Biophys Acta*, 1774, 1128-38.
14. HUANG, B. X., KIM, H. Y. & DASS, C. 2004. Probing three-dimensional structure of bovine serum albumin by chemical cross-linking and mass spectrometry. *J Am Soc Mass Spectrom*, 15, 1237-47.
15. JUAREZ, J., TABOADA, P., GOY-LOPEZ, S., CAMBON, A., MADEC, M. B., YEATES, S. G. & MOSQUERA, V. 2009a. Additional supra-self-assembly of human serum albumin under amyloid-like-forming solution conditions. *J Phys Chem B*, 113, 12391-9.
16. JUAREZ, J., TABOADA, P. & MOSQUERA, V. 2009b. Existence of different structural intermediates on the fibrillation pathway of human serum albumin. *Biophys J*, 96, 2353-70.
17. KANG, H. G., BYBEE, A., HA, I. S., PARK, M. S., GILBERTSON, J. A., CHEONG, H. I., CHOI, Y. & HAWKINS, P. N. 2005. Hereditary amyloidosis in early childhood associated with a novel insertion-deletion (indel) in the fibrinogen Aalpha chain gene. *Kidney Int*, 68, 1994-8.
18. KUMAR, S. & WALTER, J. 2011. Phosphorylation of amyloid beta (Abeta) peptides - a trigger for formation of toxic aggregates in Alzheimer's disease. *Aging (Albany NY)*, 3, 803-12.
19. LEVINE, H., 3RD 1993. Thioflavine T interaction with synthetic Alzheimer's disease beta-amyloid peptides: detection of amyloid aggregation in solution. *Protein Sci*, 2, 404-10.
20. MERLINI, G. & BELLOTTI, V. 2003. Molecular mechanisms of amyloidosis. *N Engl J Med*, 349, 583-96.
21. MILITELLO, V., CASARINO, C., EMANUELE, A., GIOSTRA, A., PULLARA, F. & LEONE, M. 2004. Aggregation kinetics of bovine serum albumin studied by FTIR spectroscopy and light scattering. *Biophys Chem*, 107, 175-87.
22. NELSON, R., SAWAYA, M. R., BALBIRNIE, M., MADSEN, A. O., RIEKEL, C., GROTHE, R. & EISENBERG, D. 2005. Structure of the cross-beta spine of amyloid-like fibrils. *Nature*, 435, 773-8.
23. PARK, K. 2012. Albumin: a versatile carrier for drug delivery. *J Control Release*, 157, 3.
24. PEPYS, M. B. 2006. Amyloidosis. *Annu Rev Med*, 57, 223-41.
25. POLVERINO DE LAURETO, P., TADDEI, N., FRARE, E., CAPANNI, C., COSTANTINI, S., ZURDO, J., CHITI, F., DOBSON, C. M. & FONTANA, A. 2003. Protein aggregation and amyloid fibril formation by an SH3 domain probed by limited proteolysis. *J Mol Biol*, 334, 129-41.

26. SUGIO, S., KASHIMA, A., MOCHIZUKI, S., NODA, M. & KOBAYASHI, K. 1999. Crystal structure of human serum albumin at 2.5 Å resolution. *Protein Eng*, 12, 439-46.
27. SUNDE, M. & BLAKE, C. 1997. The structure of amyloid fibrils by electron microscopy and X-ray diffraction. *Adv Protein Chem*, 50, 123-59.
28. SURMACZ-CHWEDORUK, W., MALKA, I., BOZYCKI, L., NIEZNANSKA, H. & DZWOLAK, W. 2014. On the heat stability of amyloid-based biological activity: insights from thermal degradation of insulin fibrils. *PLoS One*, 9, e86320.
29. TAGUCHI, K., CHUANG, V. T., MARUYAMA, T. & OTAGIRI, M. 2012. Pharmaceutical aspects of the recombinant human serum albumin dimer: structural characteristics, biological properties, and medical applications. *J Pharm Sci*, 101, 3033-46.
30. TANAKA, M., CHIEN, P., YONEKURA, K. & WEISSMAN, J. S. 2005. Mechanism of cross-species prion transmission: an infectious conformation compatible with two highly divergent yeast prion proteins. *Cell*, 121, 49-62.
31. VETRI, V., D'AMICO, M., FODERA, V., LEONE, M., PONZONI, A., SBERVEGLIERI, G. & MILITELLO, V. 2011. Bovine Serum Albumin protofibril-like aggregates formation: solo but not simple mechanism. *Arch Biochem Biophys*, 508, 13-24.
32. VISHVESHWARA, N. & LIEBMAN, S. W. 2009. Heterologous cross-seeding mimics cross-species prion conversion in a yeast model. *BMC Biol*, 7, 26.
33. VIVIAN, J. T. & CALLIS, P. R. 2001. Mechanisms of tryptophan fluorescence shifts in proteins. *Biophys J*, 80, 2093-109.
34. WANG, Y., PETTY, S., TROJANOWSKI, A., KNEE, K., GOULET, D., MUKERJI, I. & KING, J. 2010. Formation of amyloid fibrils in vitro from partially unfolded intermediates of human gammaC-crystallin. *Invest Ophthalmol Vis Sci*, 51, 672-8.
35. WUNDER, A., MULLER-LADNER, U., STELZER, E. H., FUNK, J., NEUMANN, E., STEHLE, G., PAP, T., SINN, H., GAY, S. & FIEHN, C. 2003. Albumin-based drug delivery as novel therapeutic approach for rheumatoid arthritis. *J Immunol*, 170, 4793-801.
36. ZOU, W. Q. & GAMBETTI, P. 2009. Variant Creutzfeldt-Jakob disease: French versus British. *Ann Neurol*, 65, 233-5.